groups to (acetylates) the histone proteins in adjacent nucleosomes. Gcn5 association and histone acetylation are transient; both disappear 9 hours after viral infection. Third, shortly after recruitment of Gcn5, the enhanceosome recruits the coactivator, CREB binding protein (CBP). Intriguingly, efficient CBP recruitment requires a composite surface that exists only when the enhanceosome is intact; interactions between CBP and individual activators are far less efficient in the absence of the enhanceosome (*11, 12*). Fourth, the Pol II enzyme complex is recruited by the enhanceosome at the same time as CBP is recruited. Fifth, approximately 1 to 2 hours after recruitment of the CBP–Pol II enzyme complex, the Swi-Snf nucleosome remodeling complex is recruited in a manner that depends on CBP and is strongly stimulated by histone acetylation. The recruited Swi-Snf complex disrupts the nucleosome positioned over the core promoter region, thereby permitting the transcription factor TFIID to gain access to the *IFN-β* gene, which is then switched on and transcribed (*10*).

Transcriptional activation of *IFN-β* is transient—the key feature of the regulatory switch is the programmed formation and destruction of the enhanceosome through acetylation of the architectural protein HMGI(Y) by the Gcn5 and CBP histone acetylases (*4, 13*). Acetylation of lysine at position 71 (Lys^{71}) in HMGI(Y) by Gcn5 stabilizes the enhanceosome by increasing the affinity of HMGI(Y) for the activators. In vivo, acetylation of Lys^{71} is transient, and it correlates precisely with the formation of the enhanceosome and recruitment of Gcn5. In striking contrast, CBP acetylates HMGI(Y) at Lys^{65}, which inhibits DNA-binding activity and hence destabilizes the enhanceosome. In vivo, the peak of Lys^{65} acetylation coincides with disruption of the enhanceosome. Importantly, Lys^{65} acetylation does not occur for 1 to 2 hours after CBP has been recruited to the *IFN-β* gene's promoter. Thus, Gcn5-dependent acetylation of Lys^{71} both facilities enhanceosome assembly and protects the enhanceosome by inhibiting CBP-dependent acetylation of Lys^{65}.

These findings demonstrate that the IFN-β enhanceosome uses multiple molecular mechanisms to achieve a precise on-off switch for regulating gene expression. The enhanceosome forms only when all component activators are functional. It has biochemical properties distinct from those of the individual activators, and its existence is regulated by the programmed recruitment of the Gcn5 and CBP acetylases. We still do not have enough information to assess whether cells commonly use enhanceosomes to regulate gene transcription. However, there are indications that enhanceosomes regulate the expression of several other mammalian genes (*14*) and of the Mei3 meiosis inducer gene of the yeast *Schizosaccharomyces pombe* (*15*). Thus, it is highly likely that eukaryotic organisms use modular enhancers to achieve diversity in gene expression patterns and evolutionary flexibility, and enhanceosomes to achieve regulatory precision in gene transcription.

References and Notes

1. M. Ptashne, A. Gann, *Nature* **386**, 569 (1997).
2. K. Struhl, *Cell* **98**, 1 (1999).
3. N. Munshi *et al.*, *Science* **293**, 1133 (2001).
4. K. Struhl, *Neuron* **7**, 177 (1991).
5. T. Maniatis *et al.*, *In Transcriptional Regulation*, S. L. McKnight, K. R. Yamamoto, Eds. (Cold Spring Harbor Laboratory Press, Cold Spring Harbor, NY, 1992), pp. 1193–1220.
6. D. Thanos, T. Maniatis, *Cell* **83**, 1091 (1995).
7. T. Maniatis *et al.*, *Cold Spring Harbor Symp. Quant. Biol.* **63**, 609 (1998).
8. J. Yie *et al.*, *EMBO J.* **18**, 3074 (1999).
9. J. V. Falvo *et al.*, *Mol. Cell. Biol.* **20**, 4814 (2000).
10. T. Agalioti *et al.*, *Cell* **103**, 667 (2000).
11. M. Merika *et al.*, *Mol. Cell* **1**, 277 (1998).
12. J. Yie, K. Senger, D. Thanos, *Proc. Natl. Acad. Sci. U.S.A.* **96**, 13108 (1999).
13. N. Munshi *et al.*, *Mol. Cell* **2**, 457 (1998).
14. M. Merika, D. Thanos, *Curr. Opin. Genet. Dev.* **11**, 205 (2001).
15. W. J. van Heeckeren, D. R. Dorris, K. Struhl, *Mol. Cell. Biol.* **18**, 7317 (1998).

PERSPECTIVES: COSMOLOGY

Probing Matter at the Lowest Densities

Jordi Miralda-Escudé

The lowest densities of matter in the universe are found in the vast spaces between galaxies. This tenuous intergalactic matter can only be observed through the absorption lines it produces in the spectra of bright, distant sources of light—usually quasars.

Imagine that you are observing one of these distant quasars and that several structures of intergalactic gas lie along the line of sight (see the figure). Because of the expansion of the universe, each gaseous structure recedes from us at a velocity proportional to its distance. Owing to the Doppler effect, the wavelength of a given atomic absorption line is shifted to a different observed wavelength for each of these structures. As a result, the absorption spectrum of the quasar provides us with a splendid map of the density fluctuations in the intergalactic matter along the line of sight to that quasar (*1, 2*).

For many years, this simple technique has been used to study the intergalactic medium with the Lyman-α line of atomic hydrogen (*3*) at 121.6 nm, which shifts to more easily accessible visual wavelengths for redshifts z greater than 2 (*4*). But important clues about the ionization and evolutionary history of intergalactic matter are also gained from the absorption (*5*) spectra of singly ionized helium, He II, with its Lyman-α line at 30.4 nm. The difficulty of the He II absorption is that, even with the redshift, it must still be observed in the far-ultraviolet, where Earth's atmosphere is opaque, demanding the use of space telescopes.

On page 1112 of this issue, Kriss *et al.* (*6*) report new observations of He II absorption with unprecedented resolution from the Far Ultraviolet Spectroscopic Explorer (FUSE). This new space telescope allows the He II absorption lines to be re-

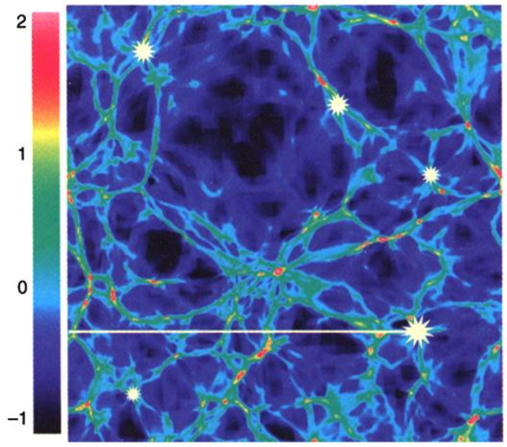

Simulated structures of intergalactic gas. The projected density in this slice from a numerical simulation shows the characteristic structures formed by gravitational collapse in the expanding universe. Left bar, logarithm of the density in units of mean density. Galaxies can form in the density peaks; supermassive black holes in their nuclei produce quasars (illustrated here as white radiant sources), which are the brightest objects in the universe. When we observe one such quasar from Earth, the gaseous intergalactic structures in the line of sight (thin white line) are detected in the absorption spectrum. The strength of the absorption reflects the density of the structure being intersected but depends also on variations in the intensity of radiation ionizing the gas due to other quasars in the vicinity of the line of sight.

CREDIT: N. GNEDIN/UNIVERSITY OF COLORADO

The author is in the Department of Astronomy, Ohio State University, Columbus, OH 43210, USA. E-mail: jordi@astronomy.ohio-state.edu

solved much better than in previous observations (*7–12*), thereby enabling detailed comparison with the hydrogen absorption lines from the same structures in the optical spectrum of the same quasar.

Most hydrogen in intergalactic space is ionized. We know this because atomic hydrogen interacts so strongly with light at the Lyman-α wavelength that, if the intergalactic matter were not ionized, it would absorb all light at wavelengths shorter than the Lyman-α line at the redshift of the source. This is because the matter in front of the source is moving away from us less rapidly than the source.

The Lyman-α absorption seen in the spectra is caused by the tiny fraction of hydrogen that is atomic. This fraction is determined by a balance of the rate of photoionization due to the ultraviolet background light from galaxies and quasars, which ionizes the atoms, and the rate of proton-electron recombinations, which create new atoms.

The same process takes place with helium. A similar balance determines the fraction of helium in the form of He II. But the remaining electron in He II is much harder to strike out than in hydrogen, requiring photons with energies higher than the ionization potential of He II, which corresponds to wavelengths shorter than 22.8 nm. These photons are not produced abundantly by galaxies, whereas many more are produced with energies above the ionization potential of hydrogen, with wavelengths less than 91.2 nm. In addition, doubly ionized helium recombines much faster than hydrogen. As a result, there is much more He II than atomic hydrogen. The He II Lyman-α absorption is therefore stronger than that of hydrogen and reveals with greater clarity the matter in the regions of lowest densities.

The comparison of the He II and hydrogen absorption made by Kriss *et al.* allows them to probe for variations of the ratio of intensities at 91.2 and 22.8 nm in the radiation background that existed in the young universe when galaxies were forming and quasars were at their most active. If the ratio between these intensities were constant in space, then so ought to be the ratio of hydrogen and He II densities. As shown by Kriss *et al.*, there is evidence for significant fluctuations in this ratio and hence for variations in the ratio of background intensities at 91.2 and 22.8 nm. Moreover, they find these variations to be present on much smaller spatial scales than it was possible to probe before.

These background fluctuations are expected to be large when luminous sources, such as quasars, are the principal sources of emission because then only a small number of sources contribute to the overall radiation intensity at any given point in space (*13–15*). The presence of a nearby luminous quasar can then greatly change this intensity by different amounts at the ionization potentials of hydrogen and He II, explaining the fluctuations. The new results of Kriss *et al.* promise important insights into the role of quasars, galaxies, and perhaps other sources, as the originators of the far-ultraviolet background in the young universe.

References and Notes

1. J. E. Gunn, B. A. Peterson, *Astrophys. J.* **142**, 1633 (1965).
2. J. N. Bahcall, E. E. Salpeter, *Astrophys. J.* **142**, 1677 (1965).
3. M. Rauch, *Annu. Rev. Astron. Astrophys.* **36**, 267 (1998).
4. The redshift z of a source is defined so that $1 + z$ is the factor by which the received light's wavelength has stretched, that is, by which the universe has expanded since the light was emitted.
5. The Lyman-α photon is actually scattered out of the line of sight, but for the purpose of the observed spectra, this is referred to as "absorption."
6. G. A. Kriss *et al.*, *Science* **293**, 1112 (2001).
7. P. Jakobsen *et al.*, *Nature* **370**, 35 (1994).
8. A. F. Davidsen, G. A. Kriss, W. Zheng, *Nature* **380**, 47 (1996).
9. D. Reimers *et al.*, *Astron. Astrophys.* **327**, 890 (1997).
10. W. Zheng *et al.*, *Astrophys. J.* **492**, 855 (1997).
11. S. F. Anderson *et al.*, *Astron. J.* **117**, 56 (1999).
12. S. R. Heap *et al.*, *Astrophys. J.* **534**, 69 (2000).
13. L. Zuo, *Mon. Not. R. Astron. Soc.* **258**, 36 (1992).
14. L. Zuo, E. S. Phinney, *Astrophys. J.* **418**, 28 (1993).
15. M. A. Fardal, J. M. Shull, *Astrophys. J.* **415**, 524 (1993).
16. I gratefully acknowledge N. Gnedin for providing the figure and for his comments on the text.

PERSPECTIVES: ISOTOPE GEOCHEMISTRY

The Origin of Water on Earth

Francois Robert

Some 4.55 billion years ago, the Sun and planets formed from the protosolar nebula, a rotating disk of gas and grains largely made of molecular hydrogen and helium. This disk is believed to have had a homogeneous isotopic composition from its center to its edge. However, the hydrogen isotopic composition of water on Earth differs widely from that of the primitive Sun. A deuterium/hydrogen (D/H) ratio of $(149 \pm 3) \times 10^{-6}$ has been estimated for the bulk Earth (*1*), compared with a solar ratio of $(20 \pm 4) \times 10^{-6}$ deduced from solar wind implanted into lunar soils (*2*) (see the first figure). This raises the problem of where the water on Earth originated.

A clue comes from carbonaceous meteorites, the most primitive objects of the solar system available for laboratory study. They contain two distinct hydrogen carriers: water, present in clay minerals, and organic hydrogen, present mostly in macromolecular structures. Chemically extracted organic matter has shown a systematic enrichment in deuterium relative to Earth, with D/H ratios up to $(380 \pm 10) \times 10^{-6}$ (*3*). In contrast, the clays, which are associated at a submicrometer scale with the organic hydrogen, had a D/H ratio close to the terrestrial ratio (see the second figure) (*4*).

The deuterium enrichment in organic matter from meteorites has been interpreted as a relic of interstellar chemical reactions that took place shortly before the planets formed. Clay minerals in some rare meteorites also exhibit deuterium enrichment, with D/H ratios up to $(720 \pm 120) \times 10^{-6}$ (*5*). In analogy with the interpretation proposed for organic matter, the origin of solar system water has been ascribed to an interstellar process. However, we do not know the actual D/H ratio in interstellar ice. The detection of deuterated ice in interstellar clouds is technically very challenging, and measurements of the D/H ratio of interstellar ice in spectra obtained by the Infrared Space Observatory are still a matter of debate (*6*). A theoretical study suggests that ice grains synthesized at 10 K in the interstellar medium through ion-molecule reactions are highly enriched in deuterium, with D/H ratios up to 10^{-2} (*7, 8*).

Observations of comets further complicate the picture. As comets approach the Sun, water vapor sublimates. Spectroscopic studies of this water vapor have revealed D/H ratios of $(310 \pm 40) \times 10^{-6}$, substantially higher than that of terrestrial water (*9*). The contribution of cometary water to terrestrial oceans should thus be small (<10%). But what caused the D/H variations in the solar system water?

Modeling studies of the evolution of the protosolar nebula (*10*) indicate that once they had entered the nebula, interstellar ice grains vaporized and the D/H ratio of the resulting deuterium-rich water vapor was lowered through isotopic exchange with molecular hydrogen. As the temperature in the nebula decreased with time, the water vapor condensed into microscopic icy grains, with decreasing D/H ratios the closer they were to the Sun. This isotopic gradient reflects the fact that the closer to the Sun, the higher the temperature and the faster the isotopic exchange between water and molecular hydrogen. As the grains grew in size, their trajectories became independent of the turbulent

The author is at the Muséum–Minéralogie CNRS, 61 Rue Buffon, 75005 Paris, France. E-mail: robert@mnhn.fr